Electronic Supplementary Material (ESI) for Journal of Materials Chemistry C.
This journal is © The Royal Society of Chemistry 2017

# Supporting Information

# Stain-induce New Phase Diagram and Unusually High Curie Temperature in Manganites

Yunfang Kou[a], Tian Miao[a], Hui Wang[b], Lin Xie[c], Yanmei Wang[a], Hanxuan Lin[a], Shasha Wang[d], Hao Liu[a], Yu Bai[a], Yinyan Zhu[a], Jian Shao[a], Peng Cai[a], Wenbin Wang[a], Haifeng Du[d], Xiaoqing Pan[c,e], Ruqian Wu*[a,b,] , Lifeng Yin*[a, f, g] and Jian Shen*[a, f, g]

---

*[a]State Key Laboratory of Surface Physics and Department of Physics, Fudan University, Shanghai 200433, China*

**Email: shenj5494@fudan.edu.cn; lifengyin@fudan.edu.cn; wur@fudan.edu.cn*

*[b]Department of Physics and Astronomy, University of California, Irvine, Irvine, CA 92697, USA*

*[c]College of Engineering and Applied Sciences, Nanjing University, Nanjing 211189, China*

*[d]High Magnetic Field Laboratory, Chinese Academy of Science, Hefei 230031, Anhui, China*

*[e]The Henry Samueli School of Engineering, University of California, Irvine, Irvine, CA 92697, USA*

*[f]Collaborative Innovation Center of Advanced Microstructures, Nanjing 210093, China*

*[g]Institute of Nanoelectronic and Quantum Devices, Fudan University, Shanghai 200433, China*

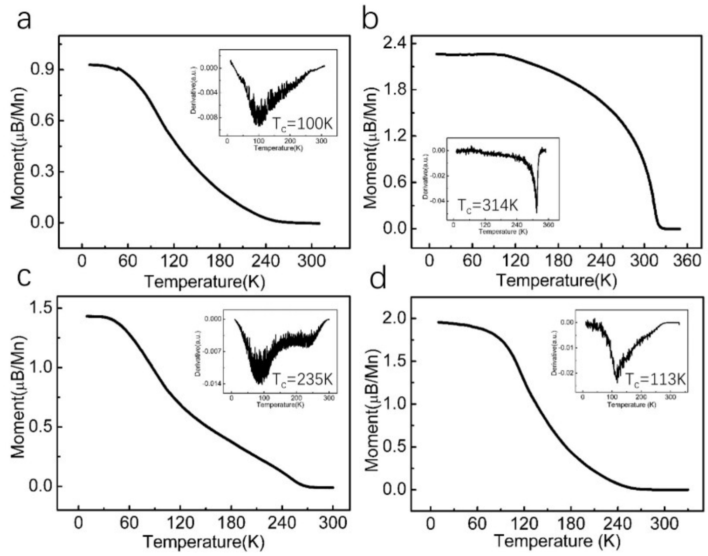


**Figure S1 | Definition of Curie temperature ($T_C$).** $T_c$ values are directly obtained from derivatives of the magnetization vs. temperature curves (insets). (a), (b), and (c) are for 30 nm $La_{1-x}Ca_xMnO_3$ thin films grown on STO (001) at x=0.15, 0.2, 0.375, respectively. (d) 210 nm $La_{0.8}Ca_{0.2}MnO_3$ thin film grown on STO (001).

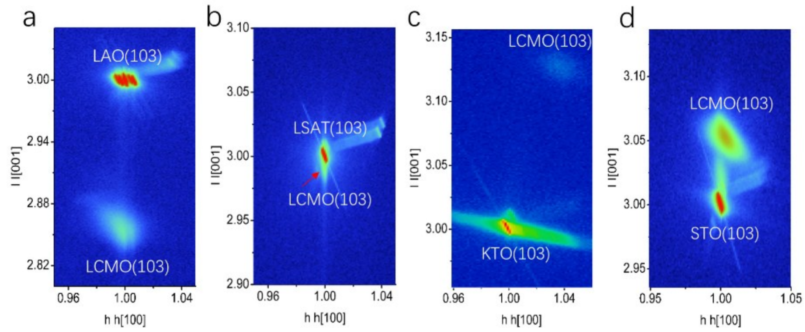


**Figure S2 | X-ray diffraction reciprocal space mapping (RSM) of the $La_{0.8}Ca_{0.2}MnO_3$ thin films.** (a), (b), and (c) are 30 nm films on LAO (001), LSAT (001), and KTO (001) substrates, respectively. (d) 210 nm film on STO (001). Note that the 30 nm film on KTO and the 210 nm film on STO (001) are partially strain relaxed.

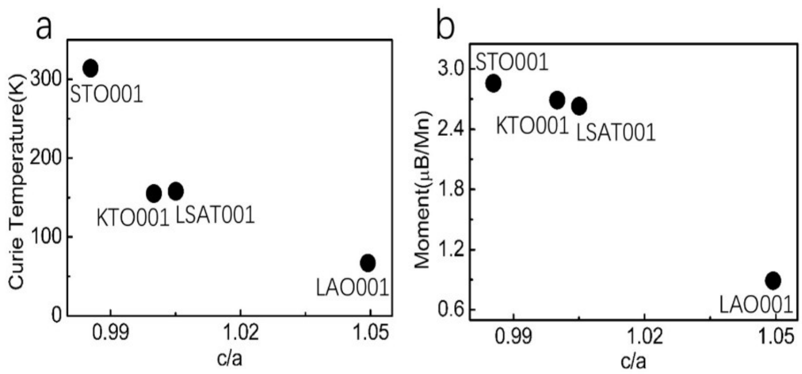


**Figure S3 | Magnetic properties of the $La_{0.8}Ca_{0.2}MnO_3$ films on different substrates.** (a) Curie temperature vs. c/a ratio. (b) Saturation magnetic moment vs. c/a ratio. Note that the c/a ratios are derived from XRD measurements.

**Figure S4 | Above room temperature magnetoresistance (MR) of Co/MgO/$La_{0.8}Ca_{0.2}MnO_3$ magnetic tunnel junctions (MTJ).** (**a**)300K, (**b**)305K, (**c**)310K, (**d**)315K, (**e**)320K, (**f**)325K. $V_{bias}$= -0.1V. The linear background is from the MR behavior of the LCMO electrode, which is subtracted to better exhibit TMR behavior in Fig.5 of main text. (**g**) MR curve of 30nm $La_{0.8}Ca_{0.2}MnO_3$ film measured at 300K.

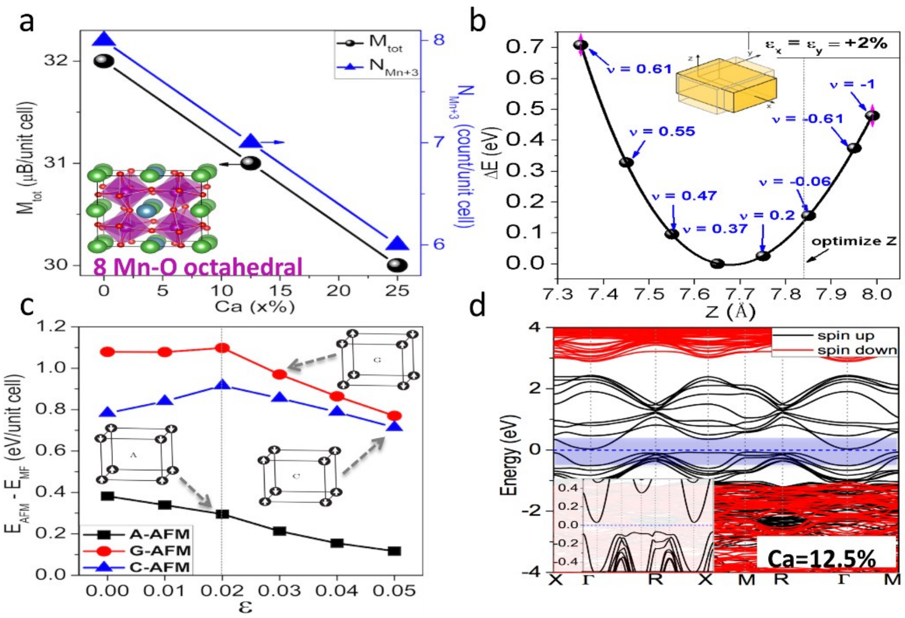


**Figure S5 | Density functional theory calculation of magnetic, electronic and mechanical properties of $La_{1-x}Ca_xMnO_3$ at different Ca concentrations.** (**a**) Ca concentration dependence of magnetic moment and $Mn^{+3}$ ions. Magnetism and $Mn^{+3}$ ions population are enhanced at low Ca concentration. (**b**) Calculated Z length dependence of total energies at fixed in-plane tensile stress ($\varepsilon_x$ = $\varepsilon_y$ = 2%) for $La_{1-x}Ca_xMnO_3$ (x=25%), the lowest total energy is obtained at Poisson ratio equal 0.37, consistent with Exp. (**c**) Calculated strain dependence of energy gap between different antiferromagnetic (AFM) and ferromagnetic (FM) configurations. Horizontal dash line

g

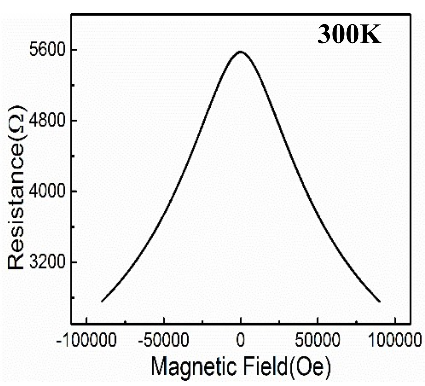


indicates the transition points at certain tensile. Insert shows different AFM configurations. (**d**) Spin-polarized electronic band structures of $La_{1-x}Ca_xMnO_3$ (x=12.5%) along high symmetry k-path, blue dash line represents Fermi level. Inset is the zoom in bands corresponding to the blue shaded area, indicating that it becomes insulator.

**Figure S6 | Magnetic properties of bulk $La_{0.8}Ca_{0.2}MnO_3$.** (a) 100Oe field cooling temperature dependent magnetization. (b) Magnetic hysteresis loops at 10K.

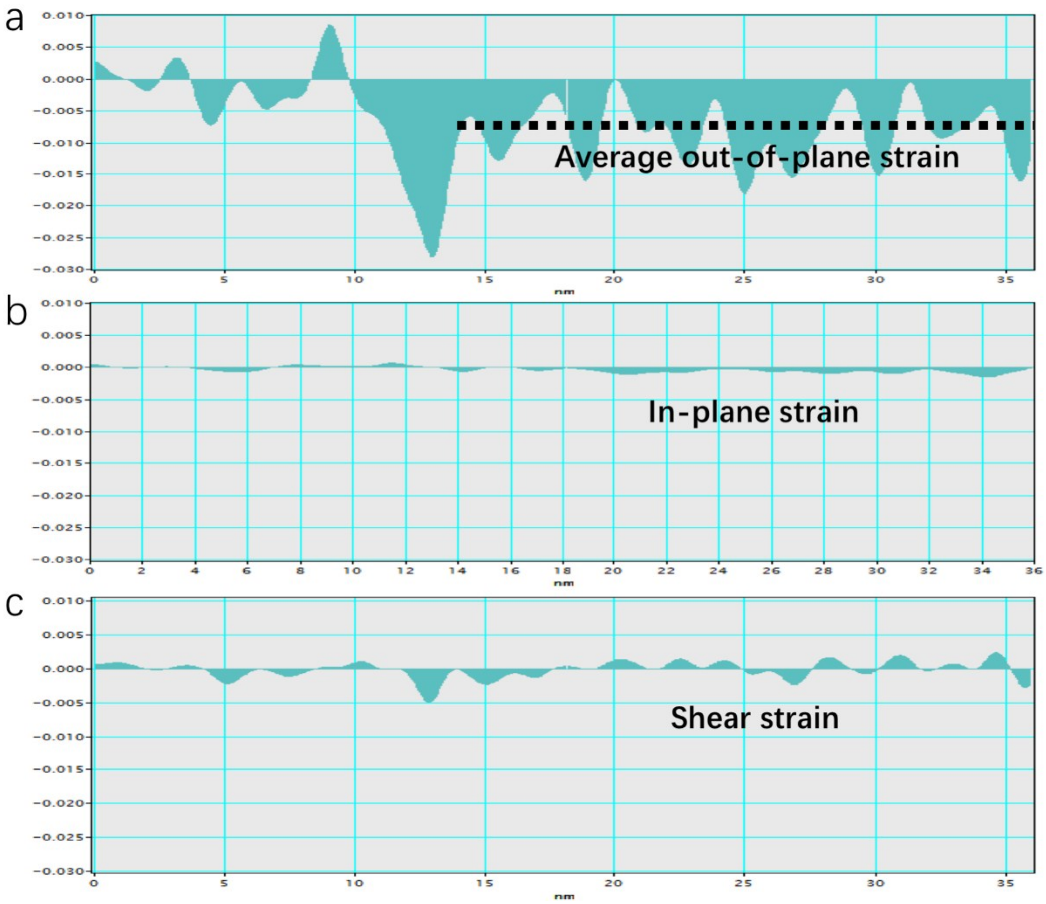


**Figure S7 | Mapping of the strain component.** (a) out-of-plane strain (b) in plane strain (c) shear strain.

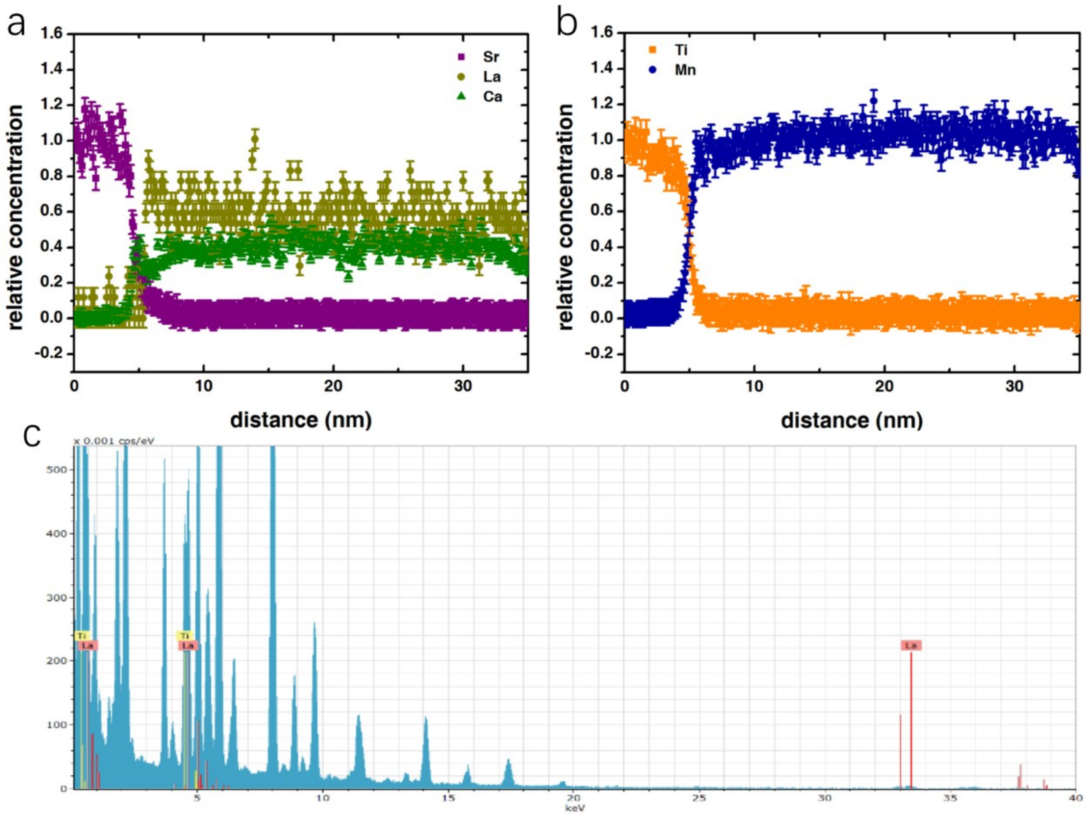


**Figure S8 | EDX mapping corresponding line profiles for each element.** (a) line profiles for Sr, La, Ca. (b)line profiles for Ti and Mn. (c) spectrum of La and Ti.

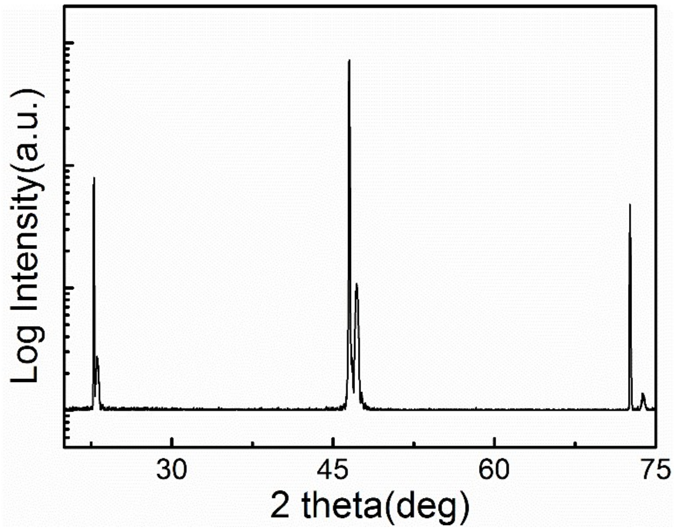


**Figure S9 | X-ray diffraction of $La_{0.8}Ca_{0.2}MnO_3$ grown on $SrTiO_3$(001).**

**Figure S10 | 100Oe field cooling temperature dependent magnetization.** (a)

$La_{0.8}Ca_{0.2}MnO_3$ grown on SrTiO3(001) at different oxygen atmosphere. (b) $La_{0.67}Ca_{0.33}MnO_3$ grown on SrTiO3(001) at different oxygen atmosphere.

**Note 1:**

The weak XRD peak near 2theta=42 degree in Figure 1c is the background signal of the specimen holder, which appears in all XRD measurements. If we change the specimen holder, the signal will disappear shown in Figure S9.

**Note 2:**

To prove the measured MR from our LCMO/MgO/Co device is indeed TMR, we measured the MR of $La_{0.8}Ca_{0.2}MnO_3$ film itself at 300K as shown in Figure S4(g). The MR of the LCMO film does not exhibit any hysteretic behavior shown by the TMR from the LCMO/MgO/Co device. The sharp peaks and lack of plateaus are caused by the fact that the coercive fields of the LCMO and Co electrodes are close at 300K.

**Note 3:**

From mapping of the out-of-plane strain component in Fig. S7a, ESI†, it is found that the out-of-plane strain at the interface is comparatively larger, while it becomes less pronounced away from the interface. In comparison, the mapping of in-plane strain component suggests that the in-plane and shear strain components are negligible as shown in Fig. S7b.c, ESI †.

**Note 4:**

As are clearly shown in the EDX spectrum, the peaks of La-L and Ti-K overlap with each other in the range about 4.5~5 kV and we have to minimize the overlapping by using La-K peak. However, the intensity of La-K peak is much lower than that of La-L peak. Because of image processing software for small intensity, we can observe some inhomogeneities in the mapping of La-K peak. In the revised version, Fig. 2d is replaced by a new image that show the mapping result by using La-L peak, which is more homogeneous compared to the result by using La-K peak. But it should be noted that there are intensities at the substrate due to the peak overlapping of La-L peak and Ti-K peak in Fig. S8 c, ESI†.